Use of dictionary learning for damage localization in complex structures

Nokhbatolfoghahai, A.; M. Navazi, H.; Groves, R. M.

DOI
10.1016/j.ymssp.2022.109394

Publication date
2022

Document Version
Final published version

Published in
Mechanical Systems and Signal Processing

Citation (APA)
Nokhbatolfoghahai, A., M. Navazi, H., & Groves, R. M. (2022). Use of dictionary learning for damage localization in complex structures. *Mechanical Systems and Signal Processing*, *180*, Article 109394. https://doi.org/10.1016/j.ymssp.2022.109394

Mechanical Systems and Signal Processing 180 (2022) 109394

Contents lists available at ScienceDirect

Mechanical Systems and Signal Processing

journal homepage: www.elsevier.com/locate/ymssp

Use of dictionary learning for damage localization in complex structures

A. Nokhbatolfoghahai [a,*], H. M. Navazi [b], R.M. Groves [a]

[a] Aerospace Non-Destructive Testing Laboratory, Faculty of Aerospace Engineering, Delft University of Technology, 2628 CD Delft, The Netherlands
[b] Ministry of Science, Research and Technology, Khovardin St., Sana't Square, Tehran, Iran

ARTICLE INFO

Communicated by Matthew Robert William Brake

Keywords:
Structural Health Monitoring
Complex structures
Lamb waves
Dictionary learning
Sparse Reconstruction

ABSTRACT

In this paper, to increase the performance of the sparse reconstruction method in real complex engineering structures an adaptive dictionary learning framework is proposed which updates the dictionary matrix, to allow improved compatibility with the complex structure. This proposed framework was developed by combining analytical modeling with training data sets and learning methods. An experimental evaluation of the proposed dictionary learning framework was performed on an anisotropic composite plate with a stiffener. In this experimental evaluation, a moving magnet was used as the artificial damage to capture the training data set, and both artificial damage in several locations and real impact damage was used for detection and location of the target damage. The obtained results confirmed the concept of the proposed dictionary learning framework for the improved health monitoring of complex structures.

1. Introduction

In recent years, structural health monitoring (SHM) has received extensive attention in aerospace industries as a way of transitioning the maintenance paradigm from scheduled maintenance to condition-based maintenance (CBM). This important task is performed by continuous real-time integrity monitoring of in-service structures and could reduce maintenance costs and provide active safety for aircraft structures [1].

Recently, the use of composite materials is expanding in aerospace and other industries due to their lightweight, high operating temperature, and increased affordability [2]. In primary aircraft structures in the maritime industry as well as for civil infrastructures, composite skin-stiffener assemblies are extensively used to reinforce the structures with the least amount of weight gain. The extended use of complex composite structures and their vulnerability to in-service damages such as barely visible impact damage (BVID) [3] increases the demand for online health monitoring of complex composite structures.

Among the various existing tools for SHM systems, the guided Lamb waves are considered to be one of the promising tools for integrity assessment of plate-like for several reasons. Guided Lamb waves systems offer relatively large coverage areas per sensor and are sensitive to small and barely visible internal and external damages [4]. Lamb wave-based SHM systems are often feasible in the inspection of inaccessible parts or those with limited access. In addition, the transducers used for generating and capturing Lamb waves are easily embedded and relatively inexpensive [5].

To perform active SHM via Lamb waves requires a network of lead zirconate titanate (PZT) actuators/sensors. The basic tasks of an

* Corresponding author.
E-mail address: A.Nokhbatolfoghahai@tudelft.nl (A. Nokhbatolfoghahai).

https://doi.org/10.1016/j.ymssp.2022.109394
Received 29 December 2021; Received in revised form 17 April 2022; Accepted 31 May 2022
Available online 18 June 2022

SHM system are damage detection and location and many researchers have focused on damage imaging methods to detect and locate failures quickly and efficiently. For this purpose, various imaging techniques based on Lamb waves and a PZT-network configuration have been developed that can be categorized as tomography [6,7], phased array techniques [8–10], and sparse array methods [11–14]. While each configuration is suitable for a specific application, sparse array imaging is particularly attractive due to its excellent coverage area per sensor and its capability of seeing damage from different angles [15].

Most of the sparse array methods extract damage features by comparing measured signals (possibly from a faulty state) with baseline signals from pristine states [6,16]. Among the sparse array-based techniques, the Delay-and-Sum (DAS) method is the most commonly used method due to its robustness and conceptual simplicity. It was developed by Wang et al. in 2004 [14] and was evolved by Michaels in 2008 [17]. However, the performance of this method tends to be poor in the presence of multiple damages or complex structures [18]. In 2013 Levine and Michaels developed an imaging method that is based on sparse reconstruction (SR) and in some cases, the images reconstructed via this method are superior to the conventional DAS [19]. Also, in 2019 and 2020 Nokhbatolfoghahai et al. developed the hybrid DAS-SR method by combining the SR method with DAS and increased the performance of these methods in case of multiple damages and under-sampled signals and they extended their developed method to anisotropic composite plates in references [20,21]. Furthermore, as this method is dictionary-based it has the potential to act as an adaptive method if some of the structural complexities could be modeled in a pre-computed dictionary matrix.

While these methods are straightforward for simple structures, in complex structures all geometric irregularities (stiffener elements, material changes, boundaries, etc.) cause waves to scatter and these multipath reflections further complicate the accurate damage detection and localization. In 2009 Clarke et al. evaluated the damage detection capability of a sparse-array Lamb-wave SHM system applied to a complex structure [12]. Using optimal baseline subtraction, he could successfully detect 5 mm and 10 mm diameter holes on a complex steel panel. Clarke and Cawley 2011 improved the defect localization capability of a Lamb-wave-based SHM system applied to a complex structure by placing a gate on signals, but at a cost in area coverage [22]. In 2011 Qui *et. al.* proposed a time-reversal focusing-based impact imaging method for impact localization in a complex composite structure [23]. They evaluated their proposed method on a composite panel with holes and stiffeners and their results showed that their method could estimate the position of impact. Qui et al. also proposed another method in 2013 [24] in which they divided a complex structure into some sub-areas and performed damage imaging in each sub-area. The complete structural image was generated by merging the images of sub-areas by considering the probability of the existence of damage in each of them. In 2015 Hall and Michaels presented a multipath guided wave imaging algorithm based on experimental and numerical simulated data in which a large number of echoes and reverberations present in recorded ultrasonic waveforms were leveraged [25]. Furthermore, Rébillat and Mechbal 2019 proposed a method based on the canonical polyadic decomposition of the Lamb wave difference signal tensor for damage localization and evaluated their method with a geometrically complex aeronautic structure [26].

Also, some previous works have focused on modeling Lamb wave propagation in complex structures [27–30], and some of them dedicated their efforts to the optimal network design for SHM of complex structures [31–33]. In addition, some previous studies have proposed a method for damage or disbound detection in the stiffener bonded to a plate [34–36].

For guided wave-based inspection of structures with complexities, there are two fundamental approaches. The first one is to construct a high-fidelity model of wave propagation based on fundamental wave equations by considering all of the geometric and material properties and boundary conditions to accurately predict the structural response to guided waves. Following this approach, several researchers have focused on analytical solutions and obtained such solutions for very specific conditions [37,38]. However, many researchers have employed numerical methods (such as a finite element) to characterize the propagation and interaction of those waves with defects [39–41]. The second approach is based on a statistical viewpoint and machine learning techniques in which, signals are captured at a random process and characterized to perform the SHM data mining procedure. This approach makes decisions purely based on prior training data sets [42,43].

While these approaches can work in some situations, for structures with high complexity, the first approach can quickly become infeasible due to the high uncertainty and intractability of analytical solutions [44] and numerical models can become too delayed to calculate for wave propagation problems. Also, in some cases, the statistical approaches tend to be impractical due to their heavy reliance on a large amount of experimental training data sets [45].

In this paper, a new method is proposed for structural health monitoring of complex structures based on sparse reconstruction and a dictionary learning framework. This method is developed by a combination of two approaches (using analytical modeling and a statistical viewpoint). In this framework, we update an initial analytically calculated dictionary by applying dictionary learning to experimentally captured guided wave data from a complex structure in the presence of multi-location artificial damages. In addition, for specific kinds of problems, a new approach is proposed to train the dictionary matrix using significantly fewer data sets in comparison with conventional dictionary learning methods. In the new approach, we locally update the elements of the dictionary matrix using the weighting matrix achieved from the training data. We also demonstrate our method with data from a non-isotropic composite plate with a bonded stiffener.

2. Theoretical background

In this section, a summary of the mathematical formulations of the sparse representation model and the dictionary learning framework for damage localization in composite complex structures are presented.

2.1. The sparse reconstruction method

In this study, sparse reconstruction (SR) refers to an imaging method for defect localization in a thin-wall structure in which the PZT transducers perform as both actuator and sensor in a pitch-catch network. This method is mainly based on the sparsity assumption of structural damages [19] which means a discretized structure is mostly undamaged and defects happen only in sparse segments of the structure. In this method, the residual signals from the structure are used and are assumed to be composed of a linear combination of scattering signals from possible damages. The residual signal of a Lamb wave which is propagated from source "*s*" and received by receiver "*r*" is calculated as:

$$R_{s.r}(t) = \widehat{S}_{s.r}(t) - \widehat{S}^{b}_{s.r}(t) \tag{1}$$

$$y_{s.r}(t) = abs(Hilbert(R_{s.r}(t))) \tag{2}$$

In the above equations, $\widehat{S}_{s.r}(t)$ and $\widehat{S}^{b}_{s.r}(t)$ are the measured and baseline signals respectively which are scaled based upon the maximum amplitude of the signal and reduced by the square root of the propagation distance as in [17] and $R_{s.r}(t)$ is the residual signal. However, since the scattering pattern is unknown and to avoid the problem of phase mismatch [15] the envelope-detected the residual signal $y_{s.r}(t)$ is used as the input to the SR method which is obtained from the absolute value of the signal analytic representation. The residual signals are decomposed into the sparse location-based components that are analytically computed from the Lamb wave propagation model as follows:

$$a(t.\theta) = \left(\frac{d}{d_{ref}}\right)^{-\frac{1}{2}} \int_{R} x'(f) e^{\frac{-i2\pi f d}{C_g(\theta)}} e^{i2\pi f t} df \tag{3}$$

$$y_{s.r}(t) = \sum\nolimits_{q=1}^{p} x_q d_{s.q.r}(t.\theta) \tag{4}$$

In Eq. (3),$a(t.\theta)$ is the far-field shape of a propagating wave after traveling a distance "d" in the direction "θ" and "d_{ref}" is the reference distance, $x'(f)$ is the Fourier transform of the excitation signal $x'(t)$, $i = \sqrt{-1}$, f is the time–frequency and $C_g(\theta)$ is the direction-dependent group velocity that is applicable in anisotropic materials [21]. Also, Eq. (4), shows the linear combination of signals from individual scattering points which is assumed to generate the residual signal $y_{s.r}(t)$. In Eq. (4), "p" shows the number of pixels in the discretized structure, and x_q is the unknown coefficient that non-zero values of it show the presence of damage in the pixel "q". In addition, $d_{s.q.r}$ is the analytically computed signal that indicates the shape of the scattering Lamb-wave that propagated from point "s" then interacts with the scatterer located at point "q" and is then received by a sensor placed at point "r". This can be calculated for an anisotropic material as follows:

$$d_{s.q.r}(t) = \left(\frac{\|r-q\|_2.\|q-s\|_2}{d_{ref}^2}\right)^{-\frac{1}{2}} \int_{R} \left\{ H(f.\theta_{s.q}.\theta_{q.r}).x'(f).e^{\frac{-i2\pi f\|q-s\|_2}{C_g(\theta_{s.q})}}.e^{\frac{-i2\pi f\|r-q\|_2}{C_g(\theta_{q.r})}} \right\} e^{i2\pi f t} df \tag{5}$$

where $H(f.\theta_{s.q}.\theta_{q.r})$ describes the interaction of the Lamb wave with damage and due to unknown prior information about the type of damage, this set is equal to 1 [15]. Also, $\theta_{a.b} = \angle(b-a)$ and $\| \|_2$ denotes the l_2-norm of a vector. By concatenation of Eq. (4) for all pairs of sensor-actuators, an underdetermined linear Eq. $\mathbf{y} = \mathbf{Dx}$ is formed which can be used to calculate the unknown sparse vector $\mathbf{x}$, using the known vector $\mathbf{y}$ of the envelope-detected residual signals and the dictionary matrix $\boldsymbol{D}$. For a distributed array of N transducers the linear Eq. $\mathbf{y} = \mathbf{Dx}$ is formed as [20]:

$$\underbrace{\begin{bmatrix} y_{1.2} \\ y_{1.3} \\ \vdots \\ y_{a.r} \\ \vdots \\ y_{N.N-1} \end{bmatrix}_{N(N-1)}}_{y} = \underbrace{\begin{bmatrix} d_{1.1.2} & d_{1.2.2} & \cdots & d_{1.i.2} & \cdots & d_{1.p.2} \\ d_{1.1.3} & d_{1.2.3} & \cdots & d_{1.i.3} & \cdots & d_{1.p.3} \\ \vdots & \vdots & \ddots & \vdots & \ddots & \vdots \\ d_{a.1.r} & d_{a.2.r} & \cdots & d_{a.i.r} & \cdots & d_{a.p.r} \\ \vdots & \vdots & \ddots & \vdots & \ddots & \vdots \\ d_{N.1.N-1} & d_{N.2.N-1} & \cdots & d_{N.i.N-1} & \cdots & d_{N.p.N-1} \end{bmatrix}_{[N(N-1)]p}}_{D} \underbrace{\begin{bmatrix} x_1 \\ x_2 \\ \vdots \\ x_i \\ \vdots \\ x_p \end{bmatrix}_{p}}_{X} \tag{6}$$

In Eq. (6) $\mathbf{y_{a.r}}$ and $\mathbf{d_{a.i.r}}$ are the vectors of discrete time-domain signals. To solve the linear inverse Eq. (6), sparse reconstruction techniques such as Basis Pursuit Denoising (BPDN), LASSO, etc. can be used.

2.2. Dictionary learning framework

In this section, we describe our framework for using dictionary learning to update our analytic dictionary for damage location on a complex structure.

Dictionary learning is a process in which a dictionary is learned using a signal training set and it has mainly two steps: the Sparse representation step and the dictionary update step. Dictionary learning has been extensively used in image processing such as for super-resolution [46], image denoising [47], and edge-detection [48]. An overview of the theory, methodology, and application of dictionary learning is provided by Tosic and Frossard [49].

In the common approach of dictionary learning for image processing, the number of training signal sets ($\mathbf{y}_{tr}$) with unknown related $\mathbf{x}_{tr}$ (the "tr" subdivisions represent training related parameters) is usually much larger than the number of dictionary atoms. An explicit and adaptive dictionary learns from large training data sets and an initial dictionary which is guessed numerically (not estimated from physics). But, in the current work, due to restrictions on the size of the experimental data that can be gathered, the number of training signal sets is much smaller than the number of dictionary atoms for which the $\mathbf{x}_{tr}$ vector for each training set is known. In addition, in our problem, an initial dictionary can be estimated well from the physical modeling of Lamb-wave propagation. To adapt the conventional dictionary learning algorithm to our conditions, we propose a modification of the conventional dictionary learning algorithm. The output of the proposed dictionary learning algorithm is an improved structured dictionary based on the well estimated initial dictionary, instead of an explicit adaptive dictionary which is the output of the conventional dictionary learning algorithm.

2.2.1. Sparse representation step

In conventional dictionary learning algorithms, if we consider training $\mathbf{x}_{tr}$ vectors as known vectors, which are sparse representations output in the first step, during the dictionary update step, only the atoms which are related to the non-zero elements of sparse vectors $\mathbf{x}_{tr}$ will be updated and the other atoms of the dictionary will not be excited. So, to cure this problem and to use the training data sets efficiently, we assume that the sparse vector $\mathbf{x}_u$ is unknown and employed the known sparse vectors $\mathbf{x}_{tr}$ indirectly in the sparse representation step. To use these known $\mathbf{x}_{tr}$ indirectly, in the sparse representation step, based on known $\mathbf{x}_{tr}$ we defined a weighting matrix $\mathbf{w}_{tr}$ and applied it to the sparse representation method as prior support information and solved the weighted sparse reconstruction in the first step of the dictionary learning framework. To define the weighting matrix $\mathbf{w}_{tr}$, we first define the probability distribution $\mathbf{E}_{tr}$ for each point in the location of $\overrightarrow{r}$ as:

$$E_{tr}(\overrightarrow{r}) = \sum_{i=1}^{N} \frac{1}{0.01 + a(|\overrightarrow{r} - \overrightarrow{r_i}|)^b} \tag{7}$$

where N is the number of non-zero atoms of the known sparse vectors $\mathbf{x}_{tr}$ and $\overrightarrow{r_i}$ is the location of the corresponding points on the structure. Also, a and b are the empirical training parameters that depend on the locations and density of training data points on structure and could be determined during the learning procedure through a trial-and-error process on the convergence of the algorithm for training data. Then, to define the training weighting matrix $\mathbf{w}_{tr}$ we use the exponential weighting function as follows [20]:

$$w_{tr}(\overrightarrow{r}) = \frac{1 + \exp(1)}{1 + \exp(1 + 10E_{tr}(\overrightarrow{r}))} \tag{8}$$

To solve this weighted sparse reconstruction problem we solve a weighted l_1 minimization using the Basis Pursuit with weight matrix (BPW) method as:

$$\mathbf{x}_u = \operatorname{argmin} \|\mathbf{x}\|_{1,\overrightarrow{w}} \text{subject to} \|\mathbf{y}_{tr} - \mathbf{D}\mathbf{x}_u\|_2 < \sigma \tag{9}$$

where σ is the user-specified parameter that should be between $0 \le \sigma < \|\mathbf{y}\|_2$. Choosing an optimal σ is not straightforward and is a trade-off between sparsity (when σ approaches to $\|\mathbf{y}\|_2$) and reconstruction fidelity (when σ goes to 0). Based on the selection of σ in previous works [15,19,50]. In this work, we set this value as a random variable in the range $0.6 \le \frac{\sigma}{\|\mathbf{y}\|_2} < 0.85$. Also $\|\mathbf{x}\|_{1,\overrightarrow{w}}$ is the weighted l_1-norm, which can be calculated as:

$$\|\mathbf{x}\|_{1,\overrightarrow{w}} = \sum_{i=1}^{n} w_i |x_i| \tag{10}$$

This trick allows the dictionary matrix to be updated locally for each training point.

2.2.2. Dictionary update step

For the dictionary updating step, there are several methods including the K singular value decomposition (K-SVD) method, the method of optimal directions (MOD), online dictionary learning (ODL), etc. MOD is one of the classical dictionary learning algorithms in which the training data are used in batches and at each iteration the whole training data is used to update the dictionary. This however causes high computational complexity and requires a large memory to keep the training data. In the K-SVD algorithm, dictionary atoms are updated one by one, so the signal SVD process is quite time-consuming. Recently, the ODL algorithm [51] has received extensive attention from researchers who mainly work in the field of image processing. This method is more efficient and uses simple mathematical operations to update the dictionary matrix and can iteratively update the dictionary using online captured data during system operation. Later we will show that the online dictionary learning method works better for our problem than the other methods.

In summary, our proposed dictionary learning framework can be explained in 5 steps:

Step 1: define training points on the structure and use magnets as moving artificial damage locations and gather experimental data for each defined training point.

Step 2: define constant values “*a*” and “*b*” of the exponential weighting function via the try and error process. It should be noted that like the other training problems, choosing the optimal training parameters is not straightforward as a closed-form formulation. However, considering the convergence behavior and validation points during the learning process, could help us to choose better training parameter.

Step 3: using the weighted sparse reconstruction method, find the sparse vector $\mathbf{x}_u$ which satisfies $\mathbf{y}_{tr} = \mathbf{D}\mathbf{x}_u$ using Eq. (8). Here $\mathbf{y}_{tr}$ are the training signals captured from the structure in the presence of moving artificial damage.

Step 4: update the dictionary matrix using the ODL algorithm using the following five steps [51]:

$$4i.\ \boldsymbol{D}=[\boldsymbol{d}_1,\cdots,\boldsymbol{d}_p]\in \boldsymbol{R}^{N(N-1)\times p}\ ,\ \boldsymbol{A}=[\boldsymbol{a}_1,\cdots,\boldsymbol{a}_p]\in \boldsymbol{R}^{p\times p}=\sum\nolimits_{i=1}^{t}\boldsymbol{x}_i\boldsymbol{x}_i^T\ ,\ \boldsymbol{B}=[\boldsymbol{b}_1,\cdots,\boldsymbol{b}_p]\in \boldsymbol{R}^{N(N-1)\times p}=\sum\nolimits_{i=1}^{t}\boldsymbol{y}_i\boldsymbol{x}_i^T\ ,\ \boldsymbol{t}(\boldsymbol{number of iteration})$$

$$4ii.\ \boldsymbol{A}_0\leftarrow 0\ ,\ \boldsymbol{B}_0\leftarrow 0\ ,\ \boldsymbol{D}_0\leftarrow \boldsymbol{initial estimated dictionary}$$

$$4iii.\ \boldsymbol{A}_t\leftarrow \boldsymbol{A}_{t-1}+\boldsymbol{x}_t\boldsymbol{x}_t^T\ ,\ \boldsymbol{B}_t\leftarrow \boldsymbol{B}_{t-1}+\boldsymbol{y}_t\boldsymbol{x}_t^T$$

$$4iv.\ \boldsymbol{D}_t\triangleq \underset{\boldsymbol{D}\in \boldsymbol{C}}{\boldsymbol{argmin}}\ \frac{1}{t}\sum\nolimits_{i=1}^{t}\frac{1}{2}\|\boldsymbol{y}_i-\boldsymbol{D}\boldsymbol{x}_i\|_2^2+\lambda\|\boldsymbol{x}_i\|_1 = = \underset{\boldsymbol{D}\in \boldsymbol{C}}{\boldsymbol{argmin}}\ \frac{1}{t}\left(\frac{1}{2}\boldsymbol{Tr}(\boldsymbol{D}^T\boldsymbol{D}\boldsymbol{A}_t)-\boldsymbol{Tr}(\boldsymbol{D}^T\boldsymbol{B}_t)\right)$$

Tooptimizefor(4)weupdatethejthcolumnandrepeatitforallcolumns.

$$4v.\ \boldsymbol{u}_j\leftarrow \frac{1}{\boldsymbol{A}_{jj}}(\boldsymbol{b}_j-\boldsymbol{D}\boldsymbol{a}_j)+\boldsymbol{d}_j$$

$$\boldsymbol{d}_j\leftarrow \frac{1}{\boldsymbol{max}(\|\boldsymbol{u}_j\|_2,1)}\boldsymbol{u}_j \tag{11}$$

where Tr represents the trace of a matrix, A_{jj} is the diagonal element of matrix $\boldsymbol{A}$, and a_j , b_j and d_j are the jth columns of matrix $\boldsymbol{A}$, $\boldsymbol{B}$, and $\boldsymbol{D}$ respectively.

Step 5: check the convergency condition according to:

$$|\mathbf{x}_u - \mathbf{x}_{tr}| < \varepsilon \tag{12}$$

Fig. 1 illustrates both the conventional and the proposed dictionary learning algorithms for comparison in a flowchart diagram.

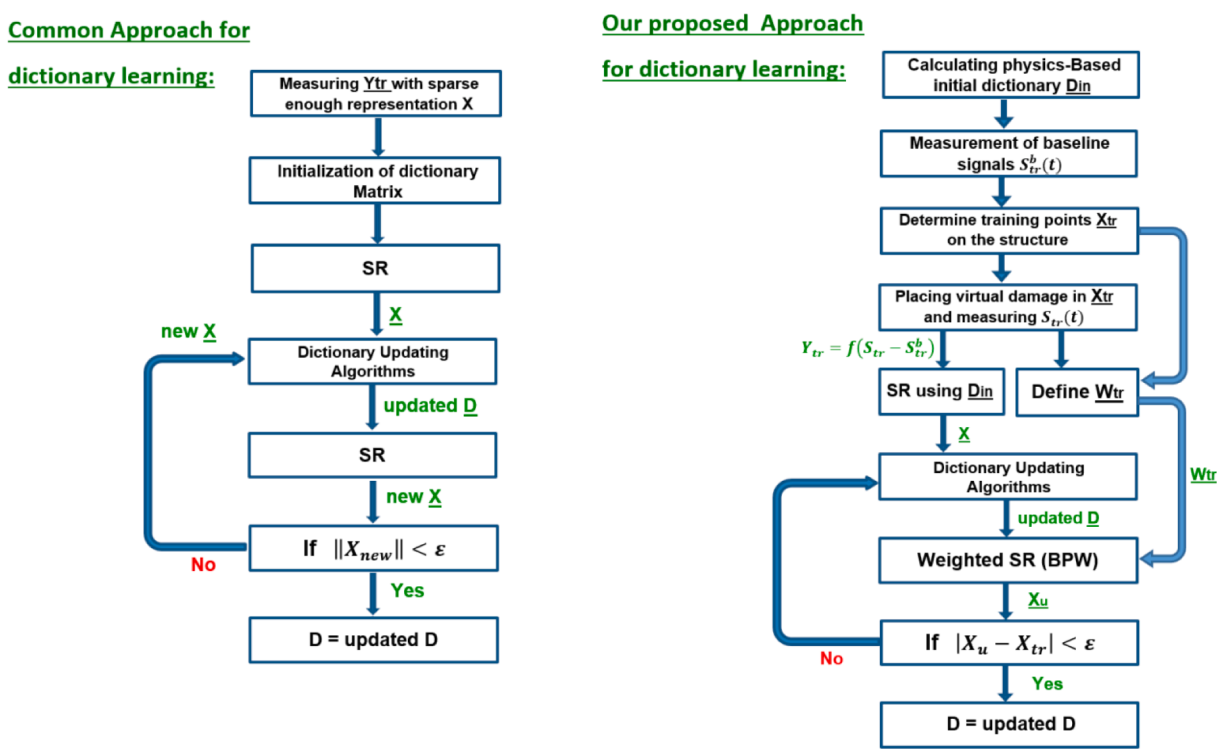

Fig. 1. Flowchart diagram of the common approach and our new approach for dictionary learning.

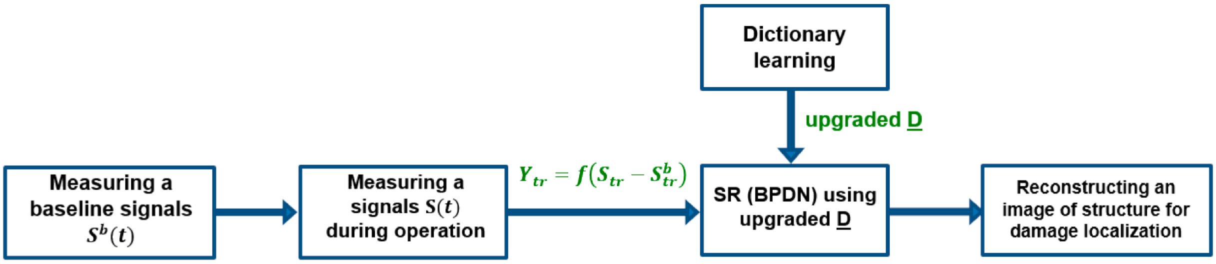

Fig. 2. Flowchart diagram of sparse reconstruction method for damage localization.

Also, after performing the dictionary learning we can use the upgraded dictionary for damage localization which is illustrated in the flowchart diagram depicted in Fig. 2.

2.3. Case study

To evaluate the performance of our new dictionary learning framework, an experimental test was performed on a composite plate with a bonded stiffener. The composite plate was manufactured using twelve unidirectional prepreg plies from AS4/8552 carbon fiber epoxy with a cross-ply layup of $[0/90]_{3S}$. The thickness of the plate after thermal curing was 2.17 mm and the plate has a size of 60 cm by 60 cm. Also, an additional stiffener with the dimension of 52 cm by 2 cm was bonded on the plate (see Fig. 3). The material properties of the prepreg used are shown in Table 1.

To generate and detect Lamb waves, the PZT transducer was used. The type of PZT is PIC 255 from Physik Instrumente (PI) with 10 mm diameter and 0.5 mm thickness were attached to the composite plate with superglue. The configuration and a picture of the specimen with the attached stiffener and PZTs and the zero-degree fiber orientation are shown in Fig. 3.

The PZT transducers act as both transmitters and receivers. To generate Lamb waves, Agilent 33500B waveform generator supplied an 80 kHz four-cycle Hann windowed tone burst signal to a wideband voltage amplifier (Agilent 33502A) to give a 40 V peak-to-peak excitation voltage to the PZT transducers. Also, to capture received signals with high quality, the output of the PZT transducers was transferred to a wideband preamplifier (MISTRAS 2/4/6C) and then digitized and recorded by a PicoScope 6402 with a 1 MHz sampling rate. Fig. 4 shows the experimental setup at the Aerospace Non-Destructive Testing Laboratory of TU Delft.

As explained above, to train the dictionary we captured data from the structure in the presence of moving artificial damage in different locations. Fig. 5(a) shows the spatial distribution of artificial damage for capturing the training data set and Fig. 5(b) shows a picture of the plate with the attached magnet (with a diameter of 6 mm) that acts as moving artificial damage.

According to the distribution of the training points and the trial and error process, the "a" and "b" constants are defined as a = 5 and b = 2. However, based on the sensitivity analysis we already performed, the sensitivity of selecting "a" in the range 3–8 does not significantly affect the final results. So, Eq. (7) is used in the form [53]:

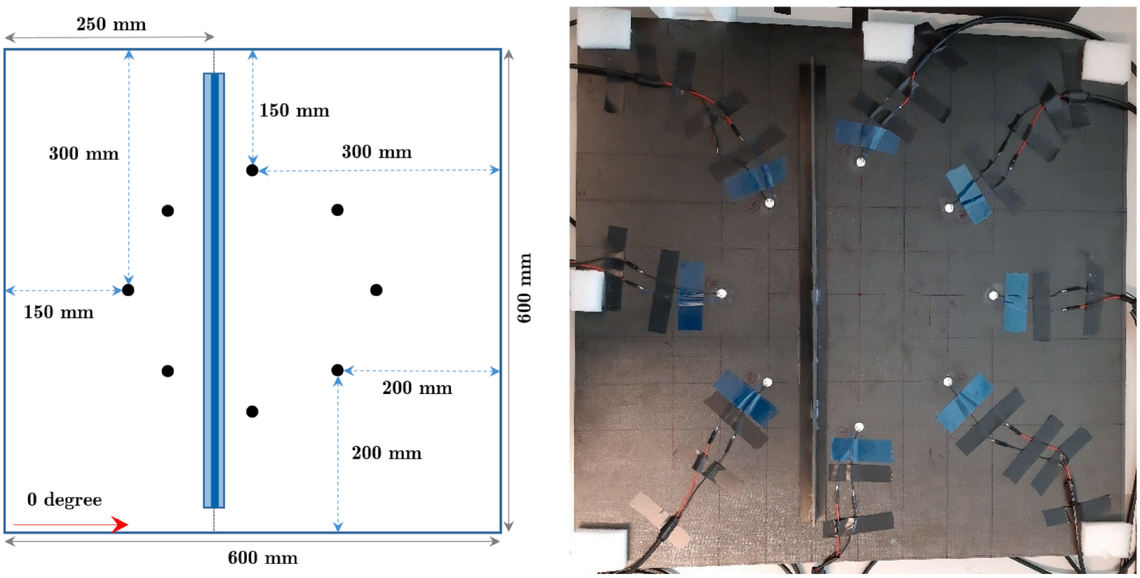

Fig. 3. Configuration of Composite plate with attached stiffener and PZTs.

Table 1
Material properties of prepreg [52].

	UD tensile strength (MPa)	UD tensile modulus (GPa)	UD compressive strength (MPa)	UD compressive modulus (GPa)	45° in-plane shear strength (MPa)	45° in-plane shear modulus (GPa)
AS4/8552	2205	141	1530	128	128	5.6

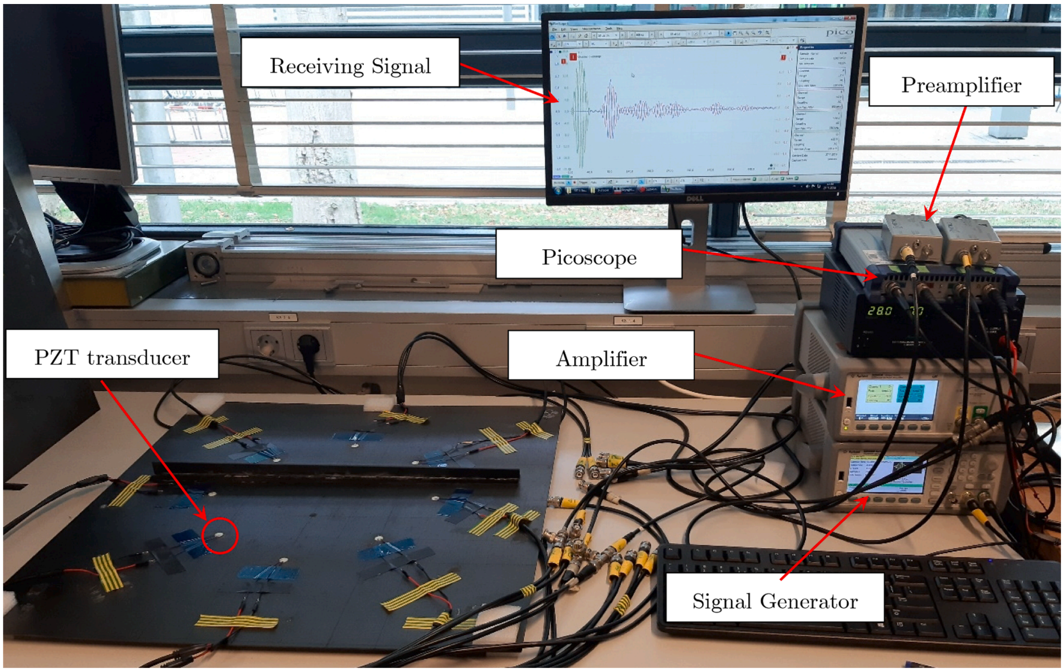

Fig. 4. The experimental setup for data gathering.

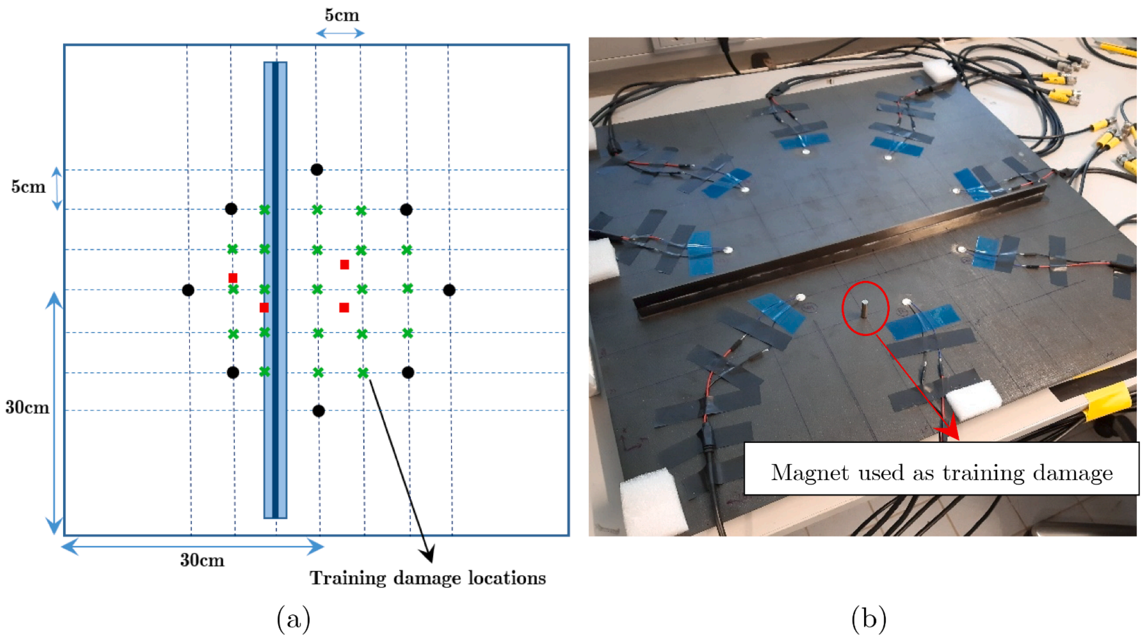

Fig. 5. (a) spatial distribution of training points (denoted by the "×" symbol) and test points (denoted by the "■" symbol) with PZTs (denoted by the "•" symbol) and stiffener configuration (b) the stiffened composite plate with attached moving magnet.

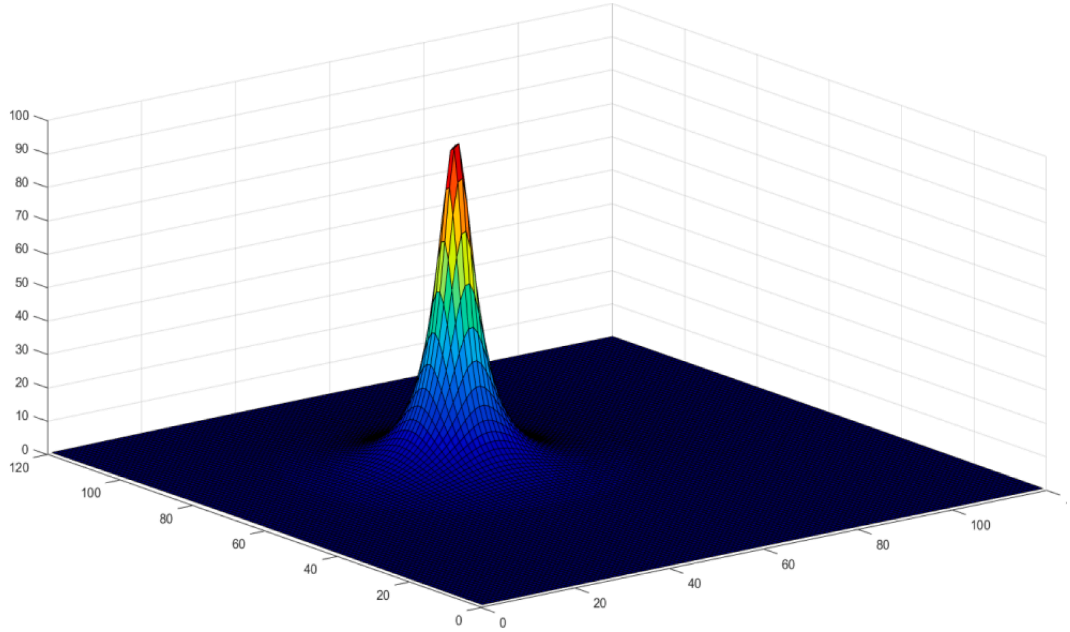

Fig. 6. probability distribution function $E_{tr}(\overrightarrow{r})$ for a typical training damage location.

$$E_{tr}(\overrightarrow{r}) = \sum_{i=1}^{N} \frac{1}{0.01 + 5(|\overrightarrow{r} - \overrightarrow{r_i}|)^2} \tag{13}$$

Fig. 6 shows the probability distribution $E_{tr}(\overrightarrow{r})$ for a typical training damage location.

After training the dictionary, the proposed algorithm was evaluated by localizing the artificial damage and then real impact damage which was placed on the structure. It should be noted that there are two types of complexity in the tested structure, which are the anisotropy of the structure and the presence of the stiffener.

3. Results and evaluation

In this section, two types of damage are detected and located on the stiffened composite plate. The first one is a magnet that acts as artificial damage and is placed in several locations. The second type of damage is impact damage that is created on the stiffened composite plate at a single location.

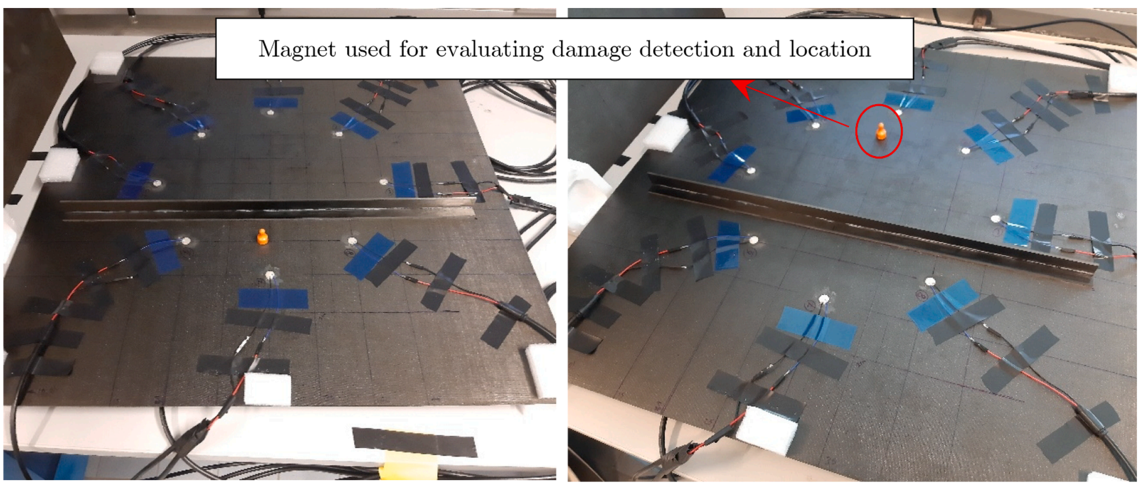

Fig. 7. The stiffened plate with artificial damage was placed at two different locations.

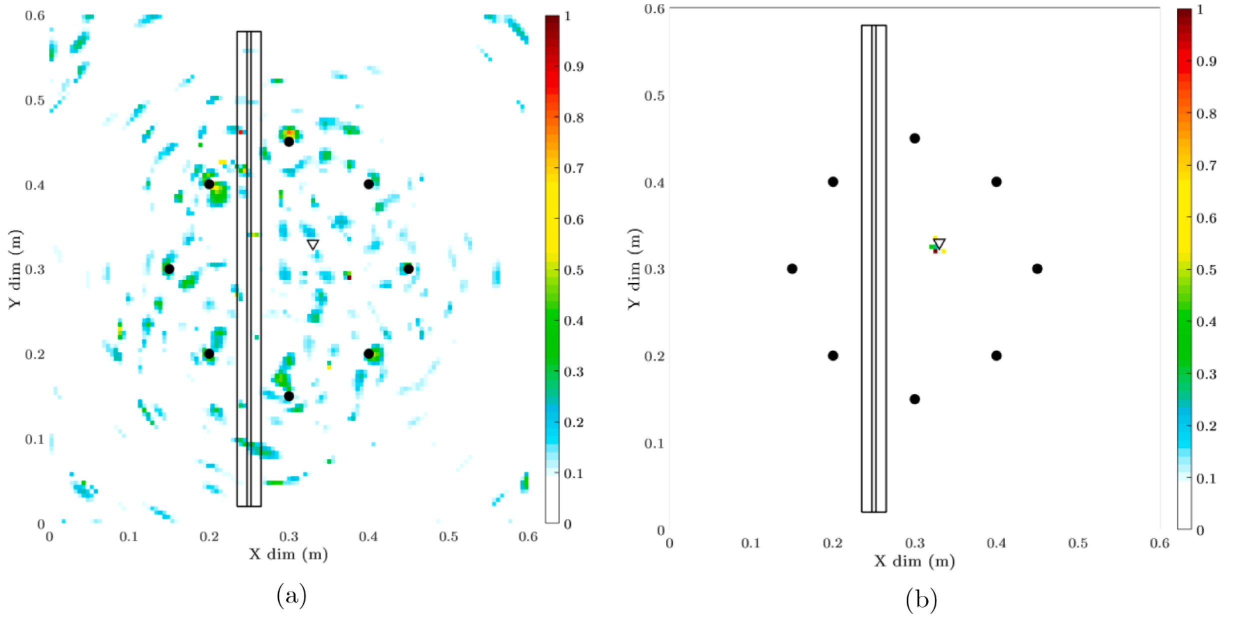

Fig. 8. Images reconstructed using the SR method with (a) the initial analytically estimated dictionary and (b) the upgraded dictionary via the dictionary learning method. Black circles denote the PZTs and the triangle shows the artificial damage location (33 cm, 33 cm).

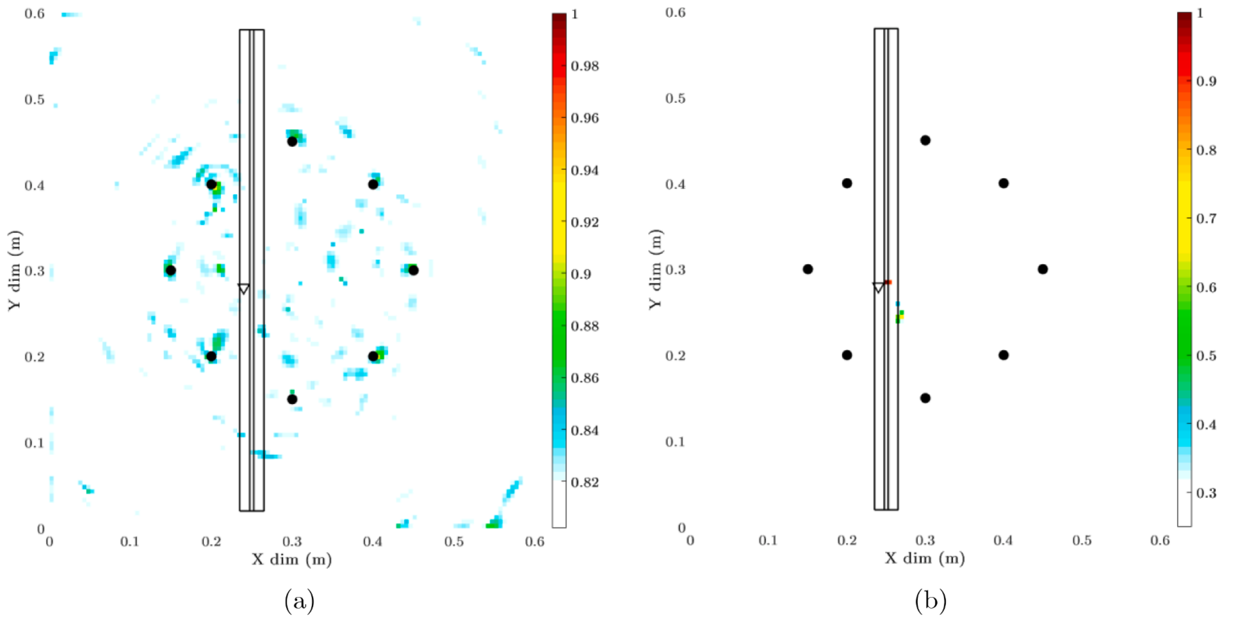

Fig. 9. Images reconstructed using the SR method with (a) the initial analytically estimated dictionary and (b) the upgraded dictionary via the dictionary learning method. Black circles denote the PZTs and the triangle shows the artificial damage location (24 cm, 28 cm).

3.1. Localization of artificial damage using the proposed learning method

In the first step, the proposed algorithm was evaluated using a magnet with a different size (with a diameter of 10 mm) and magnetic force than the one previously used for training. Also, the artificial damage was placed at different locations to the training damage locations. Fig. 7 shows the plate with the magnet attached for the evaluation of the method.

In the following, the results of the experimental tests to detect and locate artificial defects placed on a reinforced composite plate are shown. The images reconstructed using the sparse reconstruction and BPDN method for structure with artificial damage are shown in Figs. 8–11. In each figure, the result obtained from the analytically estimated dictionary (which is used as the initial dictionary in the

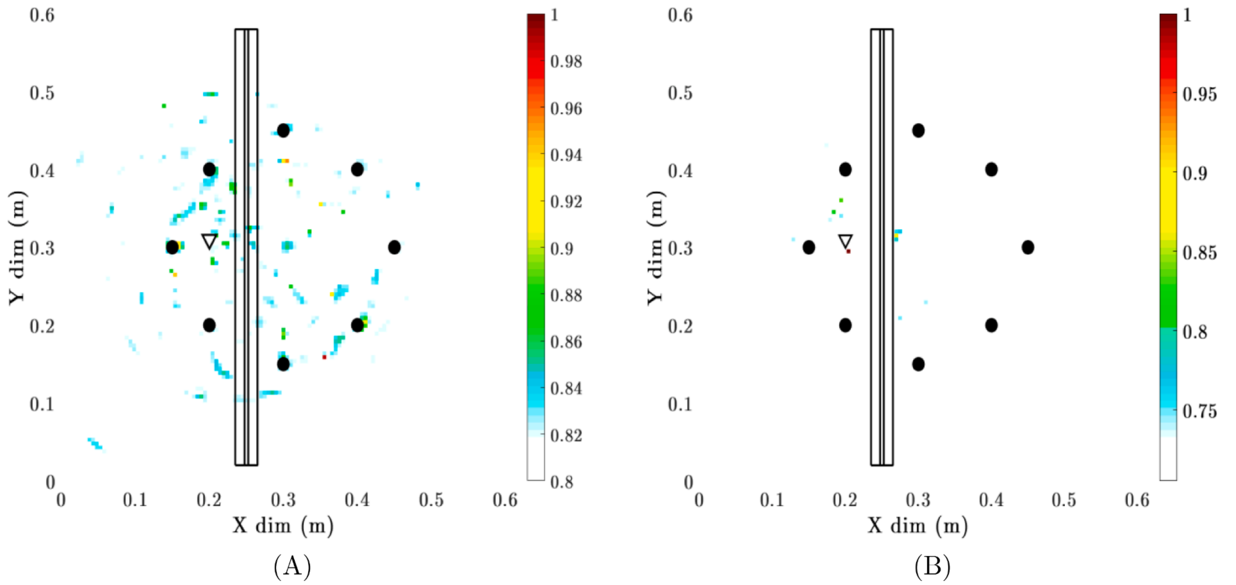

Fig. 10. Images reconstructed using the SR method with (a) the initial analytically estimated dictionary and (b) the upgraded dictionary via the dictionary learning method. Black circles denote the PZTs and the triangle shows the artificial damage location (20 cm, 31 cm).

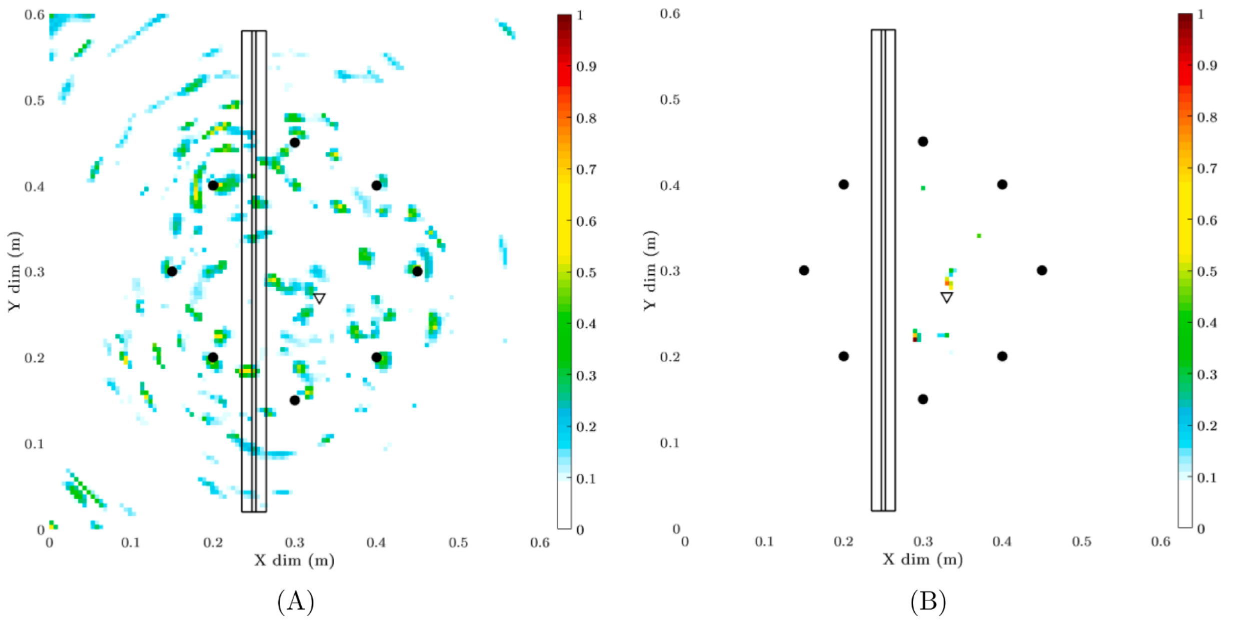

Fig. 11. Images reconstructed using the SR method with (a) the initial analytically estimated dictionary and (b) the upgraded dictionary via the dictionary learning method. Black circles denote the PZTs and the triangle shows the artificial damage location (33 cm, 27 cm).

learning procedure) is compared with the result obtained from the upgraded dictionary achieved from the proposed learning method. Also, it should be noted that due to the very small number of training data sets, the conventional dictionary learning method is not applicable and we could not achieve any meaningful results from this method.

In these figures, the symbol "∇" indicates the location of the failure, and the symbol "●" indicates the location of the PZTs.

As shown in Fig. 8, the image reconstructed by the SR method using the initial estimation dictionary matrix gives completely erroneous results in the damage detection and location. However, using the trained dictionary matrix, the damage has been detected and located with great accuracy (the error is less than 5 mm).

Also, the results shown in Fig. 9, show the success of the proposed dictionary learning algorithm in detecting and locating artificial defect locations. The noteworthy point in these experimental results is the location of the artificial failure that is placed under the stiffener. Because of this and due to the relatively high probability of failure in these areas, the results obtained in this experiment are important.

Also, the results are shown in Figs. 10 and 11 show that although there are some false detections and errors in the location of damage that occurred when using the updated dictionary, the results have still significantly have been improved. The SR method using the initial analytically estimated dictionary matrix has completely failed to detect and locate the damages.

3.2. Localization of impact damage using the proposed learning method

In the final step, the algorithm was evaluated for impact damage. The impact damage was created on the plate using the impact tower. The impact energy was 17.5 J (1.972 kg, 4.22 ms^1) and the impactor was semi-spherical with a radius of 8 mm. The impact tower and the C-scan image of the plate after impact are shown in Fig. 12.

As it is clear in Fig. 12(b) that damage is created at the impact location and in the C-scan image, the location of the PZTs and stiffener is visible. Also, the impact damage on the plate is shown in Fig. 12(c) which is barely visible.

Fig. 13 shows the images reconstructed via the SR method from the post-impacted structure. Fig. 13(a) shows the result obtained from SR using the initial analytically estimated dictionary compared with Fig. 13(b) which is the result obtained by the SR method using a trained dictionary matrix. However, due to the impact event and variations in the experimental setup, although there is some poor baseline subtraction and consequently some errors have happened in damage location, the comparison shows that the proposed learning method is still significantly improved for the detection and location of the damage compared to the initial analytically estimated dictionary.

4. Conclusion

In this work, a new approach has been proposed for the health monitoring of complex structures based on sparse reconstruction and a new dictionary learning framework. According to the results, it can be concluded that in the presence of geometric complexities in the structure, the SR method loses its efficiency without considering the structural complexities in calculating the dictionary matrix. On the other hand, in many cases, it is not possible to accurately calculate the dictionary matrix analytically considering all the structural complexities in a real structure.

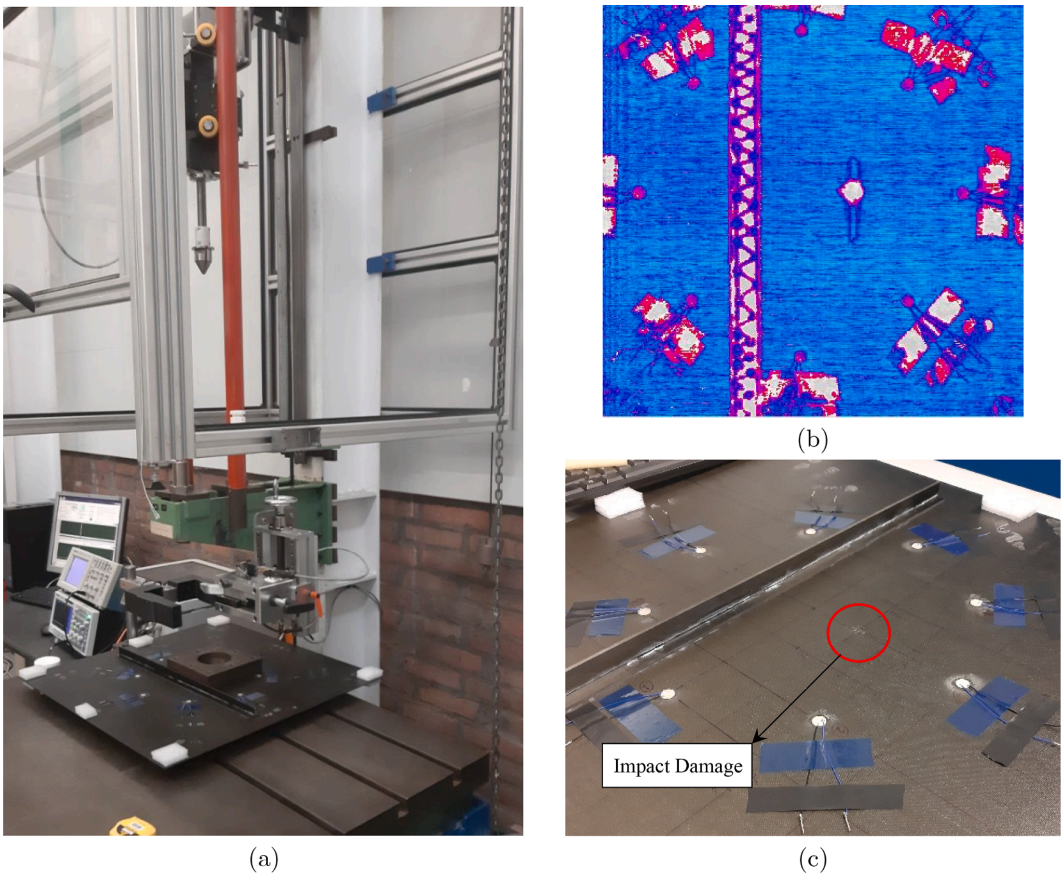

Fig. 12. (a) The impact tower with the specimen (b) The C-scan result of the post-impacted plate (c) The plate with the impact damage.

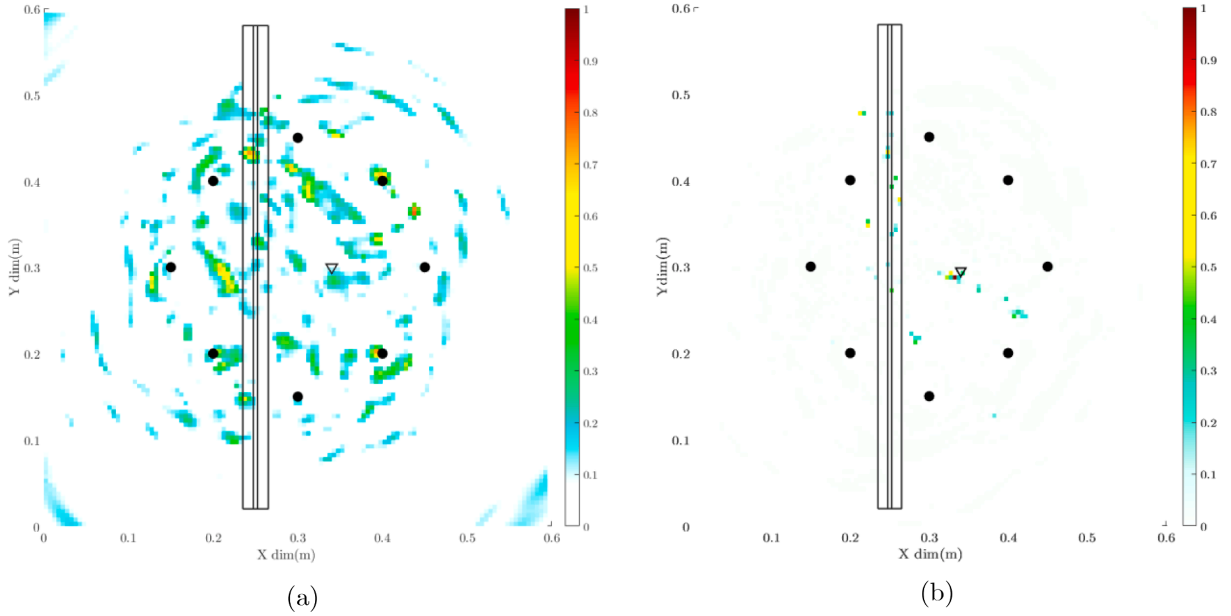

Fig. 13. Images reconstructed using the SR method with (a) the initial analytically estimated dictionary and (b) the upgraded dictionary via the dictionary learning method. Black circles denote the PZTs and the triangle shows the impact damage location (35 cm, 30 cm).

To solve this problem, in this article, a framework was proposed to update an initial rough estimated dictionary matrix adaptively using experimental data as well as the dictionary learning method.

To do this, the first challenge was the ineffectiveness of conventional dictionary learning algorithms for structural health monitoring, as most of the existing algorithms were developed based on image processing applications. In those algorithms, generating training data is low cost, and training an explicit and non-structured dictionary with a huge number of training data is possible. But in the present problem, due to the lack of access to a huge amount of training data and avoiding the time needed to develop a detailed physics-based wave propagation model, we needed to develop a new framework for dictionary learning. After developing the new framework, an anisotropic composite plate with a stiffener was used to evaluate the efficiency of the developed method for detection and location of artificial damage and real impact damage. The obtained results showed that using a trained dictionary matrix significantly improved the efficiency of the SR method in the health monitoring of complex structures. It should also be noted that although the results can confirm the feasibility of the proposed method in the laboratory, more investigation is needed to prove its applicability in larger structures.

Declaration of Competing Interest

The authors declare that they have no known competing financial interests or personal relationships that could have appeared to influence the work reported in this paper.

Acknowledgments

We gratefully thank the Sharif University of Technology for supporting part of this research as part of the doctoral dissertation of Ali Nokhbatolfoghahai (first author) under the supervision of Dr. Hossein M Navazi. We also acknowledge the AIRTuB project (Automatic Inspection and Repair of Turbine Blades) for financially supporting a part of this research which is being carried out with a Top Sector Energy subsidy from the Ministry of Economic Affairs of the Netherlands.

References

[1] Balageas, D., Fritzen, C.P. and Güemes, A. eds., 2010. Structural Health Monitoring (Vol. 90). John Wiley & Sons.
[2] V. Giurgiutiu, Structural Health Monitoring of Aerospace Composites, Academic Press, 2015.
[3] Soutis, C. and Beaumont, P.W. eds., 2005. *Multi-scale modelling of composite material systems: the art of predictive damage modelling*. Elsevier.
[4] D.N. Alleyne, P. Cawley, The interaction of Lamb waves with defects, IEEE Trans. Ultrason. Ferroelectr. Freq. Control 39 (3) (1992) 381–397.
[5] K. Balasubramaniam, Lamb-wave-based structural health monitoring technique for inaccessible regions in complex composite structures, Structural Control and Health Monitoring 5 (21) (2014) 817–832.
[6] X. Zhao, R.L. Royer, S.E. Owens, J.L. Rose, Ultrasonic Lamb wave tomography in structural health monitoring, Smart Mater. Struct. 20 (10) (2011) 105002.
[7] S.M. Prasad, K. Balasubramaniam, C.V. Krishnamurthy, Structural health monitoring of composite structures using Lamb wave tomography, Smart Mater. Struct. 13 (5) (2004) N73.

[8] P. Malinowski, T. Wandowski, I. Trendafilova, W. Ostachowicz, A phased array-based method for damage detection and localization in thin plates, Struct Health Monitor 8 (1) (2009) 5–15.
[9] L. Yu, Z. Tian, Guided wave phased array beamforming and imaging in composite plates, Ultrasonics 68 (2016) 43–53.
[10] V. Giurgiutiu, J. Bao, Embedded-ultrasonics structural radar for in situ structural health monitoring of thin-wall structures, Structural Health Monitor 3 (2) (2004) 121–140.
[11] Michaels, T.E. and Michaels, J.E., 2004, February. Sparse ultrasonic transducer array for structural health monitoring. In *AIP Conference Proceedings* (Vol. 700, No. 1, pp. 1468-1475). AIP.
[12] T. Clarke, P. Cawley, P.D. Wilcox, A.J. Croxford, Evaluation of the damage detection capability of a sparse-array guided-wave SHM system applied to a complex structure under varying thermal conditions, IEEE Trans. Ultrason. Ferroelectr. Freq. Control 56 (12) (2009) 2666–2678.
[13] J.S. Hall, J.E. Michaels, Minimum variance ultrasonic imaging applied to an in situ sparse guided wave array, IEEE Trans. Ultrason. Ferroelectr. Freq. Control 57 (10) (2010) 2311–2323.
[14] C.H. Wang, J.T. Rose, F.-K. Chang, A synthetic time-reversal imaging method for structural health monitoring, Smart Mater. Struct. 13 (2) (2004) 415–423.
[15] R.M. Levine Ultrasonic guided wave imaging via sparse reconstruction 2014 Georgia Institute of Technology USA PhD Thesis.
[16] Z. Sharif-Khodaei, M.H. Aliabadi, Assessment of delay-and-sum algorithms for damage detection in aluminium and composite plates, Smart Mater. Struct. 23 (7) (2014) 075007.
[17] J.E. Michaels, Detection, localization, and characterization of damage in plates with an in situ array of spatially distributed ultrasonic sensors, Smart Mater. Struct. 17 (3) (2008), 035035.
[18] R. Levine, J.E. Michaels, Block-sparse reconstruction and imaging for lamb wave structural health monitoring, IEEE Trans. Ultrason. Ferroelectr. Freq. Control 61 (6) (2014) 1006–1015.
[19] R.M. Levine, J.E. Michaels, Model-based imaging of damage with Lamb waves via sparse reconstruction, J. Acoust. Soc. Am. 133 (3) (2013) 1525–1534.
[20] A. Nokhbatolfoghahai, H.M. Navazi, R.M. Groves, Use of delay and sum for sparse reconstruction improvement for structural health monitoring, J. Intell. Mater. Syst. Struct. 30 (18–19) (2019) 2919–2931.
[21] A. Nokhbatolfoghahai, H.M. Navazi, R.M. Groves, Using the hybrid DAS-SR method for damage localization in composite plates, Compos. Struct. 247 (2020) 112420.
[22] T. Clarke, P. Cawley, Enhancing the defect localization capability of a guided wave SHM system applied to a complex structure, Struct. Health Monitor. 10 (3) (2011) 247–259.
[23] L. Qiu, S. Yuan, X. Zhang, Y.u. Wang, A time reversal focusing based impact imaging method and its evaluation on complex composite structures, Smart Mater. Struct. 20 (10) (2011) 105014.
[24] L. Qiu, M. Liu, X. Qing, S. Yuan, A quantitative multi-damage monitoring method for large-scale complex composite, Struct. Health Monitor. 12 (3) (2013) 183–196.
[25] J.S. Hall, J.E. Michaels, Multipath ultrasonic guided wave imaging in complex structures, Struct. Health Monitor. 14 (4) (2015) 345–358.
[26] M. Rébillat, N. Mechbal, Damage localization in geometrically complex aeronautic structures using canonical polyadic decomposition of Lamb wave difference signal tensors, Struct. Health Monitor. 19 (1) (2020) 305–321.
[27] F. Song, G.L. Huang, K. Hudson, Guided wave propagation in honeycomb sandwich structures using a piezoelectric actuator/sensor system, Smart Mater. Struct. 18 (12) (2009) 125007.
[28] A. De Luca, D. Perfetto, A. De Fenza, G. Petrone, F. Caputo, Guided wave SHM system for damage detection in complex composite structure, Theor. Appl. Fract. Mech. 105 (2020) 102408.
[29] Y. Shen, C.E.S. Cesnik, Hybrid local FEM/global LISA modeling of damped guided wave propagation in complex composite structures, Smart Mater. Struct. 25 (9) (2016) 095021.
[30] Heinze, C., Sinapius, M. and Wierach, P., 2014, July. Lamb Wave Propagation in Complex Geometries-Model Reduction with Approximated Stiffeners, 7th European Workshop on Structural Health Monitoring July 8-11, 2014. La Cité, Nantes, France.
[31] P. Ochôa, R.M. Groves, R. Benedictus, Systematic multi-parameter design methodology for an ultrasonic health monitoring system for full-scale composite aircraft primary structures, Struct. Control Health Monitor. 26 (5) (2019) e2340.
[32] N.B. Ravi, N. Chakraborty, D.R. Mahapatra, Simulation Based Optimization of Sensor Network for SHM of Complex Structures, in: In Proceeding 8th European Workshop On Structural Health Monitoring, 2016, pp. 1–7.
[33] V. Ewald, R. Groves, R. Benedictus, Integrative approach for transducer positioning optimization for ultrasonic structural health monitoring for the detection of deterministic and probabilistic damage location. *Structural Health Monitoring*, Struct. Health Monitor. 20 (3) (2021) 1117–1144.
[34] D. Samaratunga, R. Jha, S. Gopalakrishnan, Wavelet spectral finite element for modeling guided wave propagation and damage detection in stiffened composite panels, Struct. Health Monitor. 15 (3) (2016) 317–334.
[35] M.H. Sherafat, R. Guitel, N. Quaegebeur, P. Hubert, L. Lessard, P. Masson, Structural health monitoring of a composite skin-stringer assembly using within-the-bond strategy of guided wave propagation, Mater. Des. 90 (2016) 787–794.
[36] W. Roth V. Giurgiutiu April. Adhesive disbond detection using piezoelectric wafer active sensors Structural Health Monitoring and Inspection of Advanced Materials, Aerospace, and Civil Infrastructure 2015 Vol. 9437 2015 International Society for Optics and Photonics p. 94370S).
[37] F.B. Cegla, A. Rohde, M. Veidt, Analytical prediction and experimental measurement for mode conversion and scattering of plate waves at non-symmetric circular blind holes in isotropic plates, Wave Motion 45 (3) (2008) 162–177.
[38] J.C.P. McKeon, M.K. Hinders, Lamb wave scattering from a through hole, J. Sound Vib. 224 (5) (1999) 843–862.
[39] Poddar, B. and Giurgiutiu, V., 2015, March. Interaction of Lamb waves with geometric discontinuities: An analytical approach compared with FEM. In AIP Conference Proceedings (Vol. 1650, No. 1, pp. 721-730). American Institute of Physics.
[40] P.D. Wilcox, A. Velichko, Efficient frequency-domain finite element modeling of two-dimensional elastodynamic scattering, J. Acoust. Soc. Am. 127 (1) (2010) 155–165.
[41] M.Y. Bhuiyan, Y. Shen, V. Giurgiutiu, Guided wave based crack detection in the rivet hole using global analytical with local FEM approach, Materials 9 (7) (2016) 602.
[42] E.B. Flynn, M.D. Todd, A.J. Croxford, B.W. Drinkwater, P.D. Wilcox, Enhanced detection through low-order stochastic modeling for guided-wave structural health monitoring, Struct. Health Monitor. 11 (2) (2012) 149–160.
[43] Todd, M.D., Flynn, E.B., Wilcox, P.D., Drinkwater, B.W., Croxford, A.J. and Kessler, S., 2012, May. Ultrasonic wave-based defect localization using probabilistic modeling. In AIP Conference Proceedings (Vol. 1430, No. 1, pp. 639-646). American Institute of Physics.
[44] C.M. Haynes Effective health monitoring strategies for complex structures (Doctoral dissertation 2014 UC San Diego).
[45] K.S. Alguri, J. Melville, J.B. Harley, Baseline-free guided wave damage detection with surrogate data and dictionary learning, J. Acoust. Soc. Am. 143 (6) (2018) 3807–3818.
[46] S. Yang, Z. Liu, M. Wang, F. Sun, L. Jiao, Multitask dictionary learning and sparse representation based single-image super-resolution reconstruction, Neurocomputing 74 (17) (2011) 3193–3203.
[47] M. Elad, M. Aharon, Image denoising via sparse and redundant representations over learned dictionaries, IEEE Trans. Image Process. 15 (12) (2006) 3736–3745.
[48] X. Huang, F. Wu, P. Huang, Moving-object detection based on sparse representation and dictionary learning, Aasri Procedia 1 (2012) 492–497.
[49] I. Tosic, P. Frossard, Dictionary learning, IEEE Signal Process Mag. 28 (2) (2011) 27–38.
[50] A. Nokhbatolfoghahai, H.M. Navazi, R.M. Groves, Evaluation of the sparse reconstruction and the delay-and-sum damage imaging methods for structural health monitoring under different environmental and operational conditions, Measurement 169 (2021) 108495.

[51] J. Mairal, F. Bach, J. Ponce, G. Sapiro, June. Online dictionary learning for sparse coding, in: In Proceedings of the 26th annual international conference on machine learning, 2009, pp. 689–696.
[52] M. Colavita, A. Bowler, X. Zhang, P.E. Irving, Adhesively bonded CFRP straps as fatigue crack growth retarders on AA2024-T3. In: Proceedings of SAMPE Conference 2006, 2006.
[53] A. Nokhbatolfoghahai, Developing hybrid DAS-SR method for structural health monitoring using guided Lamb waves and sparse array of PZT transducers with experimental validation, Sharif University of Technology, Tehran, 2020. PhD thesis.